

Thermal Transport in a ^4He Film at the Kosterlitz-Thouless Transition

G. Agnolet, S. L. Teitel, and J. D. Reppy

*Laboratory of Atomic and Solid State Physics and the Materials Science Center, Cornell University,
Ithaca, New York 14853*

(Received 31 August 1981)

The thermal conductance of a ^4He film has been studied in conjunction with torsional oscillator measurements of the superfluid response. A dramatic rise in the thermal conductance is observed just above the Kosterlitz-Thouless transition temperature determined by the torsional oscillator. In agreement with the theoretical predictions of Ambegaokar *et al.*, the thermal conductance is found to diverge as the exponential of $(T - T_c)^{-1/2}$ for $T \rightarrow T_c^+$.

PACS numbers: 67.70.+n, 67.40.Pm

The Kosterlitz-Thouless theory of two-dimensional phase transitions¹ proposes that the low-temperature superfluid phase of unsaturated ^4He films coexists with a system of interacting vortices bound into vortex-antivortex pairs. At the critical temperature, T_c , these pairs start to dissociate into free vortices that drive the film into the normal phase. The transition is characterized by a universal discontinuous jump in the superfluid density. Observations from third-sound² and oscillating-substrate experiments (torsional pendulum³ and quartz microbalance⁴) are in good agreement with this prediction. Subsequent theoretical efforts^{5,6} have extended the equilibrium theory to include the effects of vortex dynamics. Of these, the theory of Ambegaokar, Halperin, Nelson, and Siggia (AHNS)⁵ has been particularly successful in interpreting the detailed superfluid response as measured by the torsional oscillator experiments.³

AHNS have suggested that studies of the thermal transport in superfluid films near T_c should provide a significant test of the theory. Since such measurements use a steady-state superfluid flow field to probe the behavior of the film, they complement the torsion-oscillator technique, which essentially measures the finite-frequency response of the system. Specifically, AHNS have shown that the effective thermal transport coefficient diverges as the square of the correlation length, ξ_+ , as $T \rightarrow T_c$ from above. This transport coefficient should also exhibit nonlinear behavior due to the dissociation of vortex pairs by the superfluid current. Earlier thermal transport studies in unsaturated films⁷ fail to provide any useful comparisons with the theoretical predictions. More recently several groups have reported detailed measurements of the thermal conductance of ^4He films near the superfluid transition.⁸ In this Letter we report simultaneous studies of the thermal transport and the superfluid response

as measured in a torsional oscillator. The measurements possess sufficient resolution to examine both the power and temperature dependence of the thermal conductance. The theoretical parameters derived from the conductance data are compared with those values obtained from an analysis of the torsional-oscillator data. From this comparison we can determine whether the AHNS theory provides a consistent description of the behavior of the vortices as applied to these two different dynamic regions.

The thermal conductance measurements were made in a cell constructed from materials of low thermal conductivity. The body of the cell consists of a Kapton⁹ tube 7 cm long and 0.6 cm in diameter. Within the tube a Mylar⁹ roll made from a 50-cm-long strip serves as the flow surface for the superfluid film. One end of the tube is attached to a resistive heater while the other is thermally anchored to a copper platform. Two carbon resistors, placed 4 cm apart along the side of the tube, were used to monitor the average temperature and temperature difference ΔT of the cell. Both resistors were mounted on thin copper strips which were partially embedded in the Mylar roll to insure good thermal contact to the He film. By separating the resistors from both the heater and heat sink, we avoid systematic errors from Kapitza boundary resistance and other boundary effects.

The torsional oscillator, similar to previous designs,^{10,11} is mounted on the platform directly below the conductance cell. Gas communication between the two cells is via a short tube in the platform. A third carbon resistor mounted on the body of the torsional oscillator is used to monitor the temperature of the oscillator.

Typical measurements were taken by regulating the copper platform at the desired temperature and recording the change in the thermal gradient as the heater power \dot{q} is increased. The temper-

ature difference ΔT can be measured to within a few microkelvins. Values of \dot{q} range from 100 pW to 100 μ W. Figure 1 illustrates the data obtained for a particular film coverage. ΔT is plotted as a function of the applied power \dot{q} for several temperatures in the vicinity of the transition ($T_c \sim 1.2794$ K). At the highest cell temperature, ΔT depends linearly on \dot{q} over its entire range. For slightly lower temperatures this linear relation remains valid only for small values of \dot{q} . As the temperature is further reduced the region of non-linear behavior extends to successively lower values of \dot{q} . This trend eventually reverses and a distinctly linear relation is again observed at the lowest temperatures.

The power applied at the heater induces the superfluid component of the film to flow towards the heater. In the steady state, the mass carried by the superflow is balanced by a return flow of gas. Evaporation of helium at the heater and recondensation at the heat sink constitutes the thermal transport mechanism. In the region of high thermal conductance, the viscous drag of the gas flow limits the overall thermal conductance of the system. At somewhat higher temperatures, the resistance to superflow produced by the free vortices increases to dominate the observed conductance. Eventually, as the temperature is further raised, the parallel conductance of the cell itself sets an upper bound to the thermal resistance of the system. Values for the total thermal conductance, estimated from the low-power portions of the data of Fig. 1, are plotted in Fig. 2 as a func-

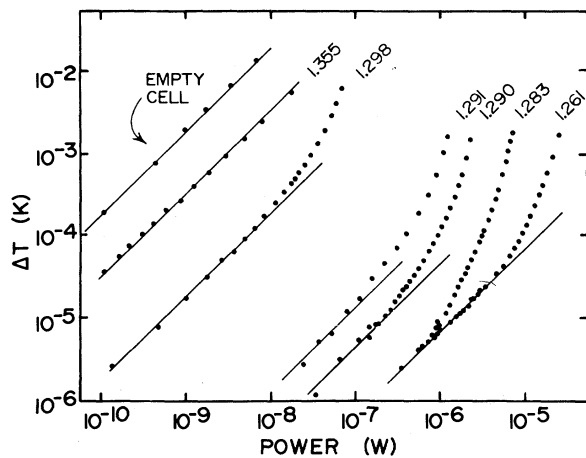


FIG. 1. The observed temperature difference ΔT plotted as a function of heater power \dot{q} for several temperatures near T_c . The solid lines serve as guides to linear behavior.

tion of temperature. In Fig. 2, we also show the period shift $2\Delta P/P$ and Q^{-1} of the oscillator which are related to the superfluid mass and dissipation of the film, respectively. The theoretical analysis of the oscillator data is made in accordance with the procedure described in Ref. 10. Although these calculations assume a constant film thickness, we believe that the effects of evaporation and film thinning do not significantly affect the interpretation of the data.¹² From the fits to the data we determine the values of $T_c = 1.2794$ K, the correlation length parameter $b = 4.9$, and the dynamic length scale $d = \frac{1}{2} \ln(14D/a^2\omega) = 12.7$. The more relevant parameter for the thermal conductance, D/a^2 , the ratio of the vortex diffusion constant to the square of the vortex core size, is then computed from the values of d and the frequency ω of the oscillator ($\omega = 8010$ sec⁻¹). For reference, the value of T_c is indicated in Fig. 2.

In analyzing the conductance data of Fig. 2, we follow AHNS⁵ and assume the flow of the superfluid component to be limited solely by the dissipative effects of free vortices moving perpendicular to the direction of the superflow. Expressing the effective conductance of the film, K_{eff} , in terms of n_f , the density of free vortices and R_g , the gas flow resistance, we have $K_{\text{eff}}^{-1} = K_{\text{film}}^{-1} + R_g$ where

$$K_{\text{film}} = \chi L S_g / (\hbar/m)^2 (D/k_B T) n_f. \quad (1)$$

S_g is the entropy per unit mass of the vapor above the film, L is the latent heat of evaporation per unit mass, and χ is a geometry factor equal to 25

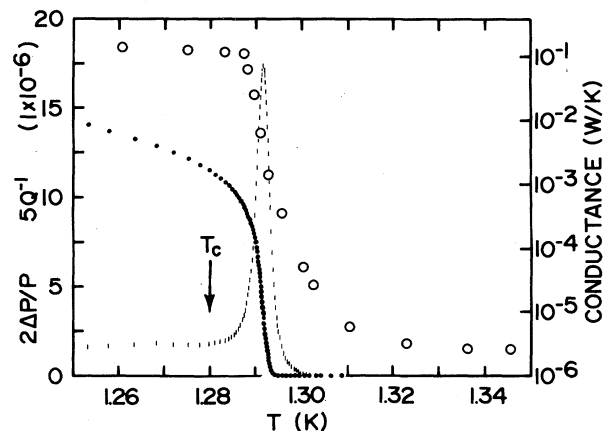


FIG. 2. The period shift $2\Delta P/P$ (closed circles) and dissipation Q^{-1} (vertical bars) of the torsional oscillator shown with the total cell conductance (open circles). The T_c indicated is obtained from fits to the oscillator data.

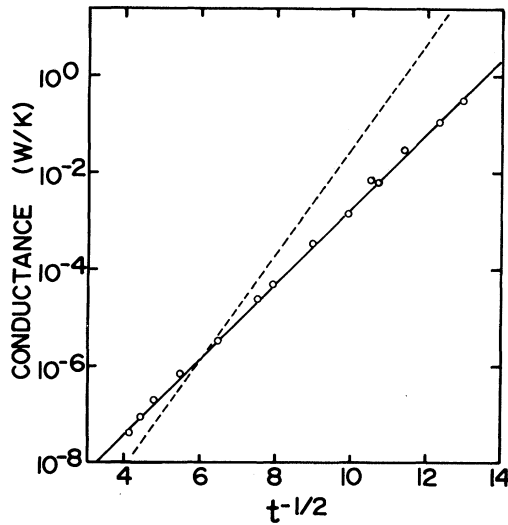


FIG. 3. The conductance K_{film} plotted as a function of $t^{-1/2}$ with $T_c = 1.2794$ K. The solid line is the fit to the data as discussed in the text. The dashed line represents the film conductance calculated from the parameters obtained from the oscillator data.

for our cell. The term R_g can be calculated if one assumes viscous flow of the gas between the Mylar layers.¹³ Combining K_{eff} with the parallel conductance of the cell we obtain the experimentally measured conductance $K_{\text{exp}} = K_{\text{eff}} + K_{\text{cell}}$.

Below T_c , there are no thermally activated free vortices and the only contribution to n_f comes from the unbinding of vortex pairs by the superfluid velocity v_s . Except in the immediate neighborhood of T_c ,¹⁴ n_f should vary as v_s^γ where $\gamma = 2 + (b/2)t^{1/2}$ and $t = |1 - T/T_c|$. Since the applied power, \dot{q} , is proportional to the rate of helium evaporation and consequently to v_s , we expect the power dependence of the conductance below T_c where $K_{\text{cell}} \ll K_{\text{eff}}$ to be given by

$$K_{\text{exp}} \simeq K_{\text{eff}} = (R_g + B\dot{q}^\gamma)^{-1}. \quad (2)$$

Although the design of the present cell is not optimized for film conduction measurements below T_c , it is possible to obtain some useful information at temperatures just below T_c . For conductivity data in this region, Eq. (2) is found to give a good description. The values obtained for R_g agree with our estimates based on the cell geometry and the gas viscosity. For reduced temperatures $t < 0.02$, we obtain from γ an average value for b of 5.1 ± 0.5 in reasonable agreement with the torsional-oscillator value.

Above T_c , the thermal conduction of the film is controlled by the presence of thermally acti-

vated free vortices. In this region, then, the film conduction is expected to diverge exponentially as T_c is approached from above^{5,13} since

$$K_{\text{film}} \propto n_f^{-1} \propto \xi_+^{-2} = a^2 \exp[(4\pi/b)t^{-1/2}]. \quad (3)$$

In Fig. 3 we test for this exponential divergence by plotting $\log K_{\text{film}}$ vs $t^{-1/2}$ where T_c is taken from the independent torsional-oscillator data. The values of K_{film} are obtained from the experimentally determined conductance together with values of the previously determined gas resistance R_g and the parallel conductance of the cell. It should be noted that these corrections only affect the data at ends of the data range.

The data shown in Fig. 3 are seen to fall on the solid straight line indicating an excellent fit to the predicted exponential form. We have also tested for a power-law fit with a less successful result. The χ^2 for the power-law fit is four times larger than that for the exponential case.

The conductivity data shown in Fig. 3 may be used to obtain values of $b = 6.9$ and $D/a^2 = 6.2 \times 10^{11} \text{ sec}^{-1}$. The values for thermal conduction calculated from the oscillator data are indicated by the dashed line in Fig. 3. In general the agreement is reasonable. However, the difference evident in Fig. 3 may point to the importance of additional influences on the vortex dynamics beyond those considered in the AHNS treatment.

The authors thank V. Ambegaokar and F. M. Gasparini for many useful discussions. One of us (J.D.R.) would like to thank the John Simon Guggenheim Memorial Foundation for Fellowship support. This work has been supported by the National Science Foundation through Grant No. DMR-77-24221 and by the Cornell Materials Science Center under Contract No. DMR-79-24008, Technical Report No. 4544.

¹J. M. Kosterlitz and D. J. Thouless, in *Progress in Low Temperature Physics*, edited by D. F. Brewer (North-Holland, Amsterdam, 1978), Vol. VIII.

²I. Rudnick, *Phys. Rev. Lett.* **40**, 1454 (1978).

³D. J. Bishop and J. D. Reppy, *Phys. Rev. Lett.* **40**, 1727 (1978).

⁴M. Chester and L. C. Yang, *Phys. Rev. Lett.* **31**, 1377 (1973).

⁵V. Ambegaokar, B. I. Halperin, D. R. Nelson, and E. D. Siggia, *Phys. Rev. B* **21**, 1806 (1980).

⁶B. A. Huberman, R. J. Myerson, and S. Doniach, *Phys. Rev. Lett.* **40**, 780 (1978).

⁷R. Bowers, D. F. Brewer, and K. Mendelssohn, *Philos. Mag.* **42**, 1445 (1951); E. Long and L. Meyer,

Phys. Rev. 98, 1616 (1955); K. Fokkens, K. W. Takonis, and R. De Bruyn Oubter, Physica (Utrecht) 32, 2129 (1960).

⁸B. Ratnam and J. Mochel, Phys. Rev. Lett. 25, 711 (1970); R. A. Joseph and F. M. Gasparini, in Proceedings of the Sixteenth International Conference on Low Temperature Physics, Los Angeles, California, 1981 [Physica (Utrecht) B, to be published]; J. Maps and R. B. Hallock, preceding Letter [Phys. Rev. Lett. 47, 1533 (1981)].

⁹Mylar and Kapton are trademarks of products marketed by the DuPont Company, Wilmington, Delaware.

¹⁰D. J. Bishop and J. D. Reppy, Phys. Rev. B 22, 5171

(1980).

¹¹G. Agnolet and J. D. Reppy, Physica (Utrecht) B & C 107, 415 (1981).

¹²An analysis of the film thinning problem and a more detailed discussion of the data below T_c will be given in a longer paper: G. Agnolet and J. D. Reppy, to be published.

¹³S. Teitel, Ph.D. thesis, Cornell University, 1981 (unpublished), and to be published.

¹⁴The criterion for the applicability of these equations is $\tau_c \gg \xi$. For our experimental parameters, we estimate $\tau_c > 200\xi$. See Ref. 5 and references therein for details.

Excitonic Mass Enhancement in Praseodymium

R. M. White^(a) and P. Fulde

Max-Planck-Institut für Festkörperforschung, D-7000 Stuttgart 80, Federal Republic of Germany

(Received 21 September 1981)

The crystal field experienced by the Pr ions in praseodymium metal produces singlet ionic ground states. The conduction electrons provide an indirect exchange coupling between the Pr ions which is not strong enough to produce long-range order but which does give rise to magnetic excitons. It is shown that these excitons contribute to the effective mass of the conduction electrons, an effect which is large and magnetic-field dependent.

PACS numbers: 72.10.Di, 71.70.Ch

Recent measurements¹ of the low-temperature specific heat of praseodymium metal suggest that the effective mass of the conduction electrons is anomalously large and magnetic-field dependent. The effect is apparently related to the presence of the $4f$ electrons, since lanthanum does not show such behavior. We show here that an effect of the observed size is expected from the contribution of the magnetic excitons to the effective mass. This represents a new mass-enhancement mechanism which should also occur in other singlet ground-state systems.

The double hexagonal-close-packed (dhcp) structure of praseodymium contains two inequivalent ionic sites, one of which has hexagonal symmetry while the other has cubic symmetry. At both sites, the crystal fields lead to singlet ground states for the Pr^{3+} ion. The system does not show magnetic order but the susceptibility is large and strongly enhanced from its single-ion value. This enhancement results from an effective Pr-Pr ion interaction which is mediated by the conduction electrons. Therefore, one might expect contributions to the electron effective mass m^* from magnetic excitons which are described by the frequency and wave-number-dependent susceptibility. These excitons are bosons,

and their contribution should be similar in character to that of paramagnons or phonons. In fact, since only the static part of the boson propagator enters into the calculation of m^* , it does not matter whether the analogy is drawn to phonons (i.e., weakly damped bosons) or paramagnons (i.e., overdamped bosons).

Let us consider a Hamiltonian of the form

$$H = H_c + H_i + H_{c-i}. \quad (1)$$

The electronic part is taken to be that of free electrons. The ionic part consists of the crystal-field Hamiltonian. The lowest excited state of the hexagonal sites is a doublet at approximately 3.2 meV. Since this is less than the first excited state of the cubic sites (8 meV), we shall restrict ourselves to the hexagonal sites. The only non-zero magnetic dipole matrix elements between the ground state $|0\rangle$ and the states $|1_s\rangle$ and $|1_a\rangle$ of the doublet are then

$$\langle 1_s | J_x | 0 \rangle = \langle 1_a | J_y | 0 \rangle = [J(J+1)/2]^{1/2} \equiv \alpha.$$

The electron-ion interaction is taken to be an isotropic exchange interaction. One has in standard notation

$$H_{e-i} = -J_{sf}(g-1) \sum_n \vec{J}_n \cdot \vec{\sigma}(R_n), \quad (2)$$